The lithosphere–asthenosphere boundary in the North-West Atlantic region

P. Kumar [a,b], R. Kind [a,c,*], W. Hanka [a], K. Wylegalla [a], Ch. Reigber [a], X. Yuan [a], I. Woelbern [a], P. Schwintzer [a,1], K. Fleming [a], T. Dahl-Jensen [d], T.B. Larsen [d], J. Schweitzer [e], K. Priestley [f], O. Gudmundsson [g], D. Wolf [a]

[a]GeoForschungsZentrum Potsdam, Telegrafenberg, 14473 Potsdam, Germany
[b]National Geophysical Research Institute, Uppal Road, Hyderabad-500007, India
[c]Freie Universität Berlin, Malteserstr. 74-100, 12249 Berlin, Germany
[d]Geological Survey of Denmark, Oster Voldgade 10, 1350 Copenhagen K, Denmark
[e]NORSAR, Institutsveien 25, 2027-Kjeller, Norway
[f]Univ Cambridge, Bullard Lab, Madingley Rise, Cambridge, CB3 0EZ, United Kingdom
[g]Danish Lithosphere Center, Oster Voldgade 10, 1350 Copenhagen K, Denmark

Abstract

A detailed knowledge of the thickness of the lithosphere in the north Atlantic is an important parameter for understanding plate tectonics in that region. We achieve this goal with as yet unprecedented detail using the seismic technique of S-receiver functions. Clear positive signals from the crust–mantle boundary and negative signals from a mantle discontinuity beneath Greenland, Iceland and Jan Mayen are observed. According to seismological practice, we call the negative phase the lithosphere–asthenosphere boundary (LAB). The seismic lithosphere under most of the Iceland and large parts of central Greenland is about 80 km thick. This depth in Iceland is in disagreement with estimates of the thickness of the elastic lithosphere (10–20 km) found from postglacial rebound data. In the region of flood basalts in eastern Greenland, which overlies the proposed Iceland plume track, the lithosphere is only 70 km thick, about 10 km less than in Iceland which is located directly above the proposed plume. At the western Greenland coast, the lithosphere

* Corresponding author. GeoForschungsZentrum Potsdam, Telegrafenberg, 14473 Potsdam, Germany Tel.: +49 331 288 1240; fax: +49 331 288 1277.

E-mail addresses: prakashngri@rediffmail.com (P. Kumar), kind@gfz-potsdam.de (R. Kind), hanka@gfz-potsdam.de (W. Hanka), wyle@gfz-potsdam.de (K. Wylegalla), yuan@gfz-potsdam.de (X. Yuan), woelbern@gfz-potsdam.de (I. Woelbern), kevin@gfz-potsdam.de (K. Fleming), tdj@geus.dk (T. Dahl-Jensen), tbl@geus.dk (T.B. Larsen), johannes@norsar.no (J. Schweitzer), keith@esc.cam.ac.uk (K. Priestley), og@dlc.ku.dk (O. Gudmundsson), dasca@gfz-potsdam.de (D. Wolf).

[1] Has passed away on Dec. 2004.

thickens to 100–120 km, with no indication of the Iceland plume track identified. Below Jan Mayen the lithospheric thickness varies between 40 and 60 km.

Keywords: Lithosphere–asthenosphere boundary; Iceland; Greenland; S-receiver functions

1. Introduction

High-viscosity lithospheric plates moving over a lower-viscosity asthenosphere is a basic element of plate tectonics. Lithosphere and asthenosphere are originally mechanical definitions with regards to their reaction to forces acting over thousands or millions of years [1]. However, additional usages of the term 'lithosphere' have been introduced since then: thermal, seismic or chemical [2]. Obtaining high-resolution seismic observations of the litho-sphere–asthenosphere boundary (LAB) is not an easy task. Observations of low seismic velocities in the upper mantle are interpreted as being indicative of the asthenosphere. The first seismic observations of an 'asthenospheric channel' were obtained by Gutenberg [3] at about 100 km depth. Therefore, seismologists sometimes call the LAB the 'Gutenberg discontinuity' (mostly in oceanic regions). The lithosphere is seis-mologically divided into two parts, the crust and the mantle lithosphere, the latter being the high-velocity lid on top of the asthenosphere. However, high-reso-lution seismic body-wave observations of the LAB are very rare. This is in contrast to the Moho, which is globally a much better documented discontinuity. So far, most information about the thickness of the lith-osphere comes from low-resolution surface-wave observations (e.g. [4]). The thickness of the litho-sphere is considered to be close to zero at mid-ocean ridges, about 200 km beneath stable cratons, with 80–100 km being the global average. Thybo and Perchuc [5] suggest the existence of a global zone of reduced velocity at about 100 km depth underlying continental regions, based on controlled source seis-mic data. Li et al. [6] and Kumar et al. [7] obtained detailed maps of the LAB around the Hawaiian island chain and in the Tien Shan–Karakoram region, respec-tively, using the S-receiver function technique [8]. This new technique complements the traditional S to P conversion method (applied to S or SKS phases)

and adds a few more processing steps. Such steps are, as in the P-receiver function technique, source equal-isation by deconvolution and distance move-out cor-rection. Both steps are applied in order to enable the summation of events from different distances and with different magnitudes and source-time functions. This technique works very well, enabling observations of the LAB with a resolution so far only known for the Moho.

In this work we determine the lithospheric thick-ness for Iceland, Greenland and the island of Jan Mayen. Greenland is a continent of Precambrian age (see [9] for a discussion of Greenland geology). Darbyshire et al. [10] observed a thickening of the lithosphere from 120 to 200 km going from east to west in southern Greenland using the surface wave technique.

Iceland is thought to be one of the classic mantle plumes [11] interacting with a mid-ocean ridge, al-though this view is disputed [12]. The crustal thick-ness (up to 45 km) is several times thicker than that expected for oceanic crust (e.g. [13,14]). White and McKenzie [15] concluded that the large thickness of the Icelandic crust is a result of magmatic intrusions. The mechanical lithosphere of Iceland is thought to be very thin (10–20 km), judging from rapid postglacial uplift [16]. A 10–20 km thick lithosphere would mean that the lower crust and Moho are located within the asthenosphere. There are also arguments that east Iceland may be a continental splinter [17–19]. Seismic surface-wave studies have furthermore found indica-tions of a 50–110 km thick lithosphere under parts of Iceland [18,20,21]. Evans and Sacks [22] found be-tween Iceland and Jan Mayen a lithospheric thickness of 50 km from surface wave data, typical for young oceans. Vinnik et al. [23] have shown a negative discontinuity at a depth of 80 km beneath all of Ice-land, using essentially the same data and technique that we have used here. Jan Mayen is a small volcanic island located about 600 km north of Iceland and

about 400 km east of Greenland on the Jan Mayen fracture zone. It is considered to be a micro continent [24].

2. Data and observations

For the Greenland study, we used seismic data from the GLATIS and NEAT experiments [25,26]. During these experiments, seismic stations were deployed along the Greenland coast and on the ice sheet for periods ranging from several months to several years. For Iceland, we used the publicly available data of the ICEMELT and HOTSPOT experiments [27,28]. In addition, we used data from permanent IRIS [29] and GEOFON [30] stations, and from two seismic stations on the island of Jan Mayen: JMI, operated by the Norwegian National Seismic Network (http://www.Ifjf.uib.no/Seismologi/nnsn/nsninfo2.html) and JMIC, operated by NOR-SAR [31]. The locations of the stations and of the S-P piercing points at 80 km depth are shown in Figs. 1–3. Since converted phases are usually weak signals, a number of records must be summed to obtain a good signal-to-noise ratio. We defined non-overlapping regions on Greenland, Iceland and Jan
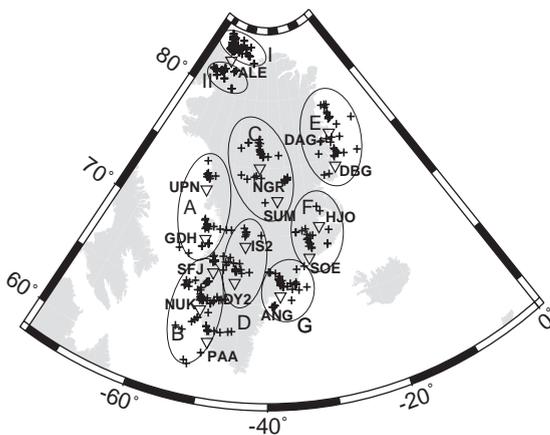

Fig. 1. Location of the temporary and permanent seismic stations of the GLATIS and NEAT experiments, and of IRIS and GEOFON in Greenland (and one in NE Canada, ALE) used in this study (reversed triangles), and of the piercing points of the S-receiver functions at 80 km depth (plus signs). The regions used for the summation of seismic traces have also been marked and are labelled A–F and I, II.
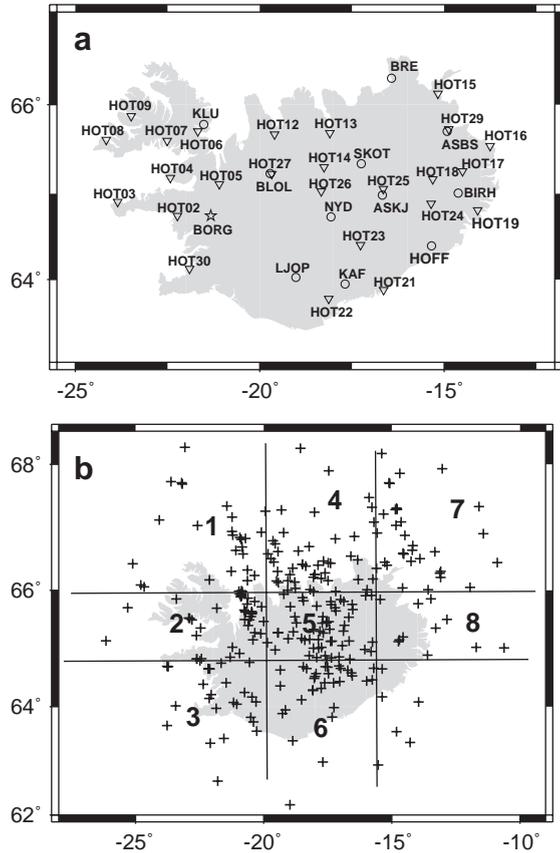

Fig. 2. a) Location of the temporary seismic stations of the HOT-SPOT and ICEMELT experiments and of the IRIS station BORG. b) Location of the piercing points of the S receiver functions at 80 km depth. Also marked are the regions (1–8) used for the summation of the seismic traces.

Mayen, where all traces with piercing points in these regions have been summed to form one record that is representative for the entire region (see Figs. 1–3). The number of traces stacked within each region are more than 20 (see Figs. 1, 2, and 3a). Individual traces (not summed traces) are shown in Fig. 3b for the Jan Mayen stations as an example of the quality of our data. The individual S-receiver functions and its stacks are also shown from the region 2 in Iceland (Fig. 4a), and from the region C in Greenland (Fig. 4b).

Fig. 5a shows the summation traces of the P component for all regions. Zero time is the S-arrival time, where negative times indicate the period prior to the S arrival. We have rotated the ZNE components into the RTZ system using the theoretical backazi-
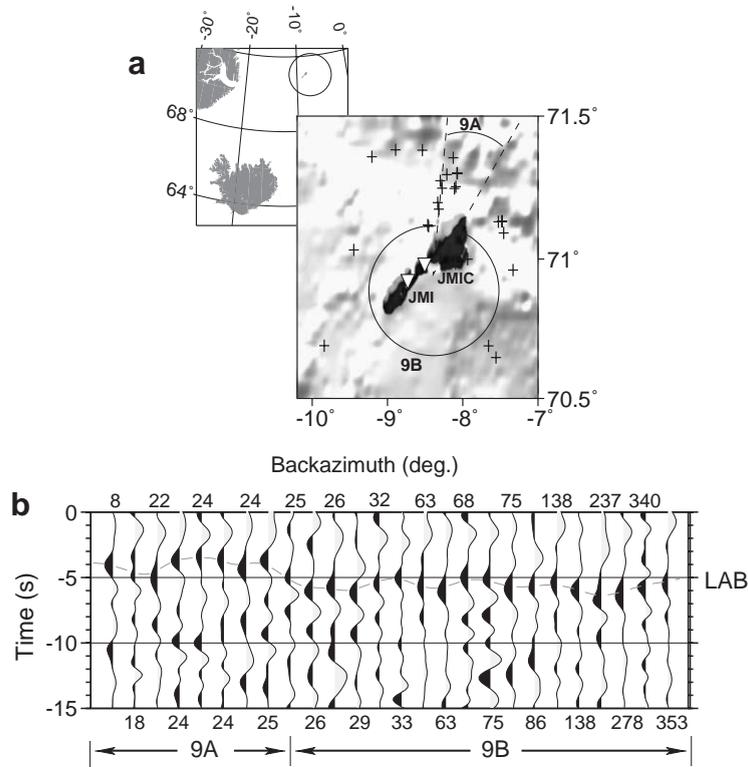
Fig. 3. a) Location of the seismic stations JMI and JMIC of the Norwegian National Seismic Network (JMI) and of NRSAR (JMIC) on the island of Jan Mayen and of the piercing points of the S-receiver functions used. Also marked are two regions, 9A and 9B, that were used for the summation of seismic traces. b) Individual (not summed) S receiver functions observed at the Jan Mayen stations. The LAB is clearly observed in all traces. Events with backazimuths of 8–25°(region 9A) show the LAB earlier then the events arriving from all other azimuths (region 9B).
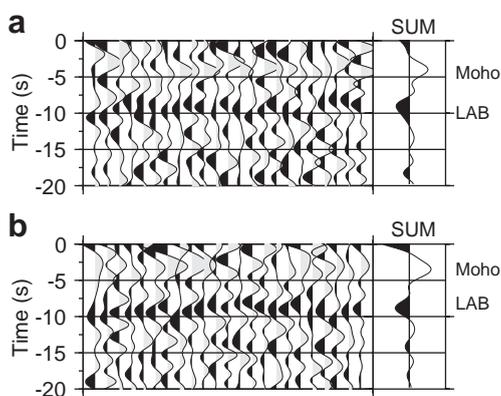

Fig. 4. The individual S-receiver functions from Iceland and Greenland and the corresponding stacked traces on the left. (a) is from the region 2 in Iceland (Fig. 2) and (b) is from the region C in Greenland (Fig. 1). These two plots clearly show the presence of coherent negative phases at around 8 to 9 s. The small scatter in the data (about 0.5 s) are a source of errors in depth determination.

muth angle. R and Z are then rotated a second time into the P-SV system. The angle of incidence is defined by the minimum of energy in the P component at the arrival time of the S phase. All traces are distance moveout corrected before summation, using a reference slowness of 6.4 s/deg based on the IASP91 global reference model [32]. A bandpass filter of 4–20 s has been applied. Two precursor phases are clearly visible in Fig. 5a, the Moho and a second phase, which we term the LAB. The arrival times of the Moho and LAB must be measured at the maximum (or minimum) of the signal due to the deconvolution. The arrival times of the LAB in seconds may be multiplied by a factor of 10 (according to the IASP91 model) to obtain the LAB depth estimate in kilometers. The possible sources of errors in depth determination are primarily from the time to depth conversion (due to the uncertainty in lithospheric velocity) and the selection of the times of the
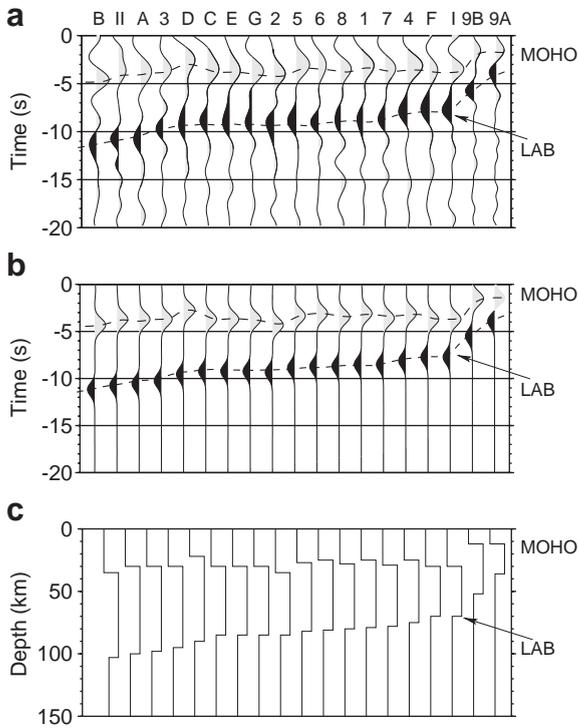
Fig. 5. a) S-receiver functions in the NW Atlantic obtained at seismic stations on Greenland, Iceland and Jan Mayen. Zero is the arrival time of the S phase. Negative times indicate the period prior to the S-signal arrival. Characters on top of the figure indicate the regions used for the summation of the seismic traces. The location of these regions is shown in Fig. 2. Two seismic phases are marked: the crust–mantle boundary (Moho) and the lithosphere–asthenosphere boundary (LAB). The traces are sorted by the arrival times of the LAB phase. The time scale is valid for a move out correction slowness of 6.4 s/degree. Multiplication of the LAB times by a factor of 10 gives approximately the LAB depth. b) Theoretical receiver functions of the S velocity models in c). Moho and LAB are the only two phases predicted by the model (no multiples). The velocities are kept fixed in all models in c) (Vs crust=3.58 km/s, Vs lithospheric mantle lid=4.5 km/s, Vs asthenosphere=3.9 km/s). Only the depth of both the discontinuities are varied to fit the travel times.

phases due to scattering (~0.5 s) in the data. Here, we estimated the maximum error bounds due to the various uncertainties as being less than about 10 km for the depth estimation. The signs of the Moho and the LAB are opposite, indicating downward increasing and decreasing velocity jumps, respectively. The traces in Fig. 5a are sorted according to the arrival times of the LAB. Characters on the top correspond to the regions (see Figs. 1–3). The clearness of the LAB

in Fig. 5a is especially remarkable, since phases in the uppermost mantle are difficult to observe at a high resolution using other techniques. In P-receiver functions, the time window of the LAB arrival is heavily disturbed by crustal reverberations. These reverberations are not present in the S-receiver functions, because the converted phases are S precursors, whereas multiples arrive after the main phase. The Moho is usually well observed in P-receiver functions, which have shorter periods and therefore higher resolution. Hence, we will concentrate here on the LAB phase. It should be noted that stations on the Greenland Ice Sheet (regions C and D) produce nearly undisturbed S-receiver functions in contrast to P-receiver functions, which are heavily disturbed by reverberations in the ice layer [25]. In Fig. 5b,c we have modelled the observed data presented in Fig. 5a using theoretical seismograms (Fig. 5b), the models used are displayed in Fig. 5c. Complete theoretical seismograms are computed (plane-wave Haskell-matrix formalism) using simple models consisting of a homogeneous crust on top of a homogeneous mantle lithosphere, both overlaying a homogeneous asthenosphere. However, we have not modelled the sharpness of the LAB. Only the depths of the Moho and of the LAB have been adjusted to fit the different arrival times of both phases in different regions. We believe this simple modelling, which is sufficient to reproduce all features of the S precursors (in S-receiver functions), provides evidence for the interpretation of the observed phase called LAB as the lithosphere–asthenosphere boundary.

A map of the LAB depth, as determined from the data, is shown in Fig. 6. The LAB is 80 km deep under most of Iceland and large parts of Greenland (yellow in Fig. 6). In Iceland, we have only two regions where the LAB differs from 80 km depth, region 3 (90 km, light blue) and region 4 (70 km, light red). Along the west coast of Greenland, the LAB is at 100–120 km depth (dark blue). North of Greenland, in the transition to the Arctic Ocean, the LAB shallows from 120 km (dark blue) to 70 km (light red). The shallowest LAB on Greenland is observed in region F (70 km, light red). The Jan Mayen LAB varies between 40 and 60 km depth (dark red) and is clearly the shallowest observed in this study. Details of the Jan Mayen LAB are given in Fig. 3b. A surprising result is that the entire
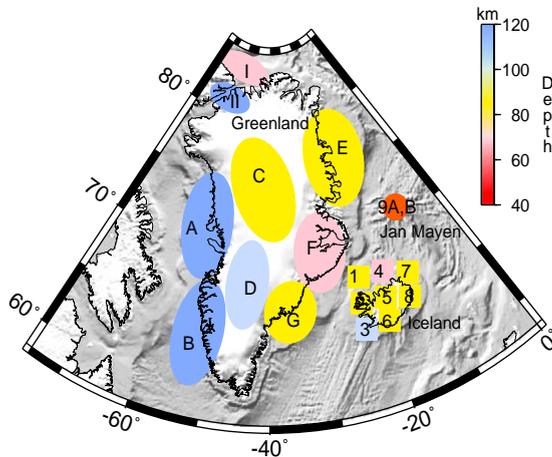
Fig. 6. Bathymetric map of the NW Atlantic with regions marked where the depth of the lithosphere was obtained by the S-receiver functions. Location of seismic stations and of piercing points of S receiver functions at the LAB are shown in Figs. 1–3.

Icelandic LAB has practically the same depth as large parts of central Greenland.

3. Discussion and conclusions

Similar to our results, Li et al. [6] and Kumar et al. [7] have also observed the LAB in Hawaii and in the Tien Shan–Karakoram area, respectively. These findings lead us to suppose that the LAB may be a globally existing and observable discontinuity, comparable to the Moho. The S-receiver function technique therefore appears to be a very useful tool for mapping the global LAB.

However, as mentioned above, there are different usages of the phrase 'lithosphere'. In seismology, a velocity decrease marks the lower boundary of the lithosphere, whereas the mechanical thickness of the lithosphere may be estimated from other data, such as postglacial rebound observations. In Iceland, these data sets give different results. Glacial-isostatic adjustment (GIA) studies infer that the viscosity stratification underlying Iceland consists of a thin elastic lithosphere overlying a low-viscosity asthenosphere. For example, Sigmundsson [16], using post-glacial sea-level observations and assuming a 10 km elastic lithosphere (the approximate maximum depth of earthquakes in SW-Iceland), estimated an upper

limit of 1×10^{19} Pa s for the underlying viscosity. Sigmundsson and Einarsson [33], from an assessment of lake-tilt data resulting from the melting of the Vatnajoekull Ice Cap, inferred a sub-lithosphere viscosity of between $1 \times 10^{18} - 5 \times 10^{19}$ Pa s. More recently, Thoma and Wolf [34] used present-day changes in uplift and gravity to propose thicknesses of 10 to 20 km for the lithosphere, and a viscosity range of $7 \times 10^{16} - 3 \times 10^{18}$ Pa s for the asthenosphere viscosity. Similar values are given by Sjoeberg et al. [35], based on GPS campaign results from around Vatnajoekull. The result of a 50–100 km thick seismic lithosphere beneath Iceland, as seen in seismic surface-wave data and in S-receiver function data, therefore appears to conflict with these estimates of the elastic lithosphere thickness (10–20 km). To examine how we may reconcile the two estimates, Fig. 7 presents predictions of vertical uplift rates around Vatnajoekull based on a range of earth models that
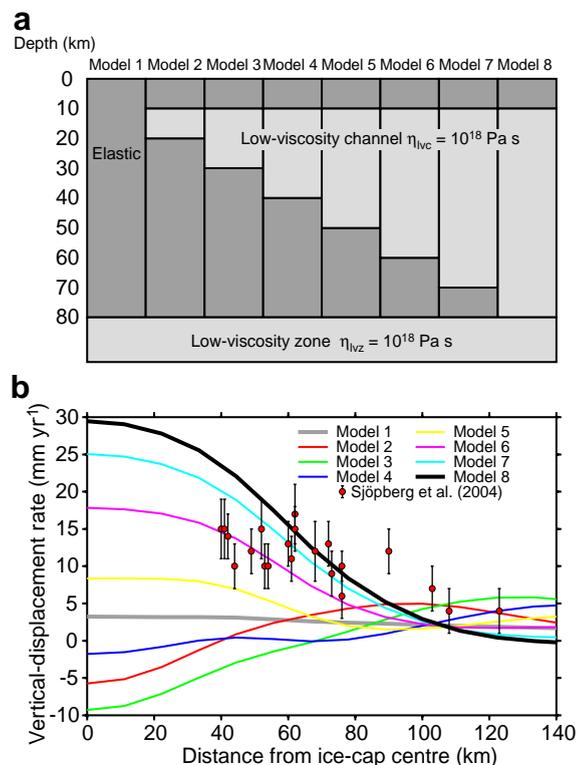

Fig. 7. a) The earth models used to examine the possibility that the 80 km discontinuity represents a lower elastic layer bounding a low-viscosity channel. b) The predicted and measured [38] vertical uplift rates from the centre of the Vatnajoekull Ice Cap.

incorporate a low-viscosity channel within the seismic lithosphere, as well as earth-model end members with lithosphere thicknesses of 80 and 10 km. Although a detailed parameter space study was not carried out, our assumed viscosity (10^{18} Pa s) is of a similar order of magnitude as values found from other studies (e.g. $0.3–2 \times 10^{19}$ Pa s [36], 1992; $3 \times 10^{18} – 3 \times 10^{19}$ Pa s [37]). These results are compared with recent GPS-based up-lift rates [38]. Model 6, with a channel thickness of 50 km, gives a reasonable fit to the observations. However, an alternative explanation of this discrepancy may be that the seismic lithosphere, reacting to short term (seconds or minutes) elastic forces, is not related to the elastic lithosphere reacting to longer term (years to thousands of years) forces.

The suggested track of the Iceland plume in Greenland is marked by tertiary flood basalts in our regions F and A (Fig. 6, [9,39]). The lithosphere in region F is the thinnest for Greenland (70 km) while region A, which is located at the west coast, shows a lithosphere thickness of about 120 km (Fig. 6). This could mean that the track of the Iceland plume is traceable to the east coast of Greenland, but not to the central part or the west coast, where the lithosphere has possibly had enough time to regain its normal thickness. This could also mean that the Iceland plume has caused, in a manner similar to the Hawaii plume, a delayed rejuvenation of the lithosphere (starting from our observed 80 km lithosphere at Iceland) when the plate passed over it. In Fig. 8, the residual geoid signal in the NW-Atlantic is shown, obtained from a combination of the most recent CHAMP [40]and GRACE [41] satellite data with aerogravimetry and terrestrial gravity data from the Arctic Gravity Project (ArcGP, [42]) after all geoid features larger than 2500 km were filtered out. We note positive residual geoid heights over the Iceland hotspot as well as in our region F at the east coast of Greenland. There is no continuation of these positive residual heights across Greenland to the flood basalt region at the west coast (region A). The larger positive anomaly in southern Greenland remains unexplained. The thinning of the lithosphere in eastern Greenland (region F in Fig. 8b) is clearly visible. The thinning occurs in the mantle part of the lithosphere, not in the crust, because the Moho in region F is not updoming.
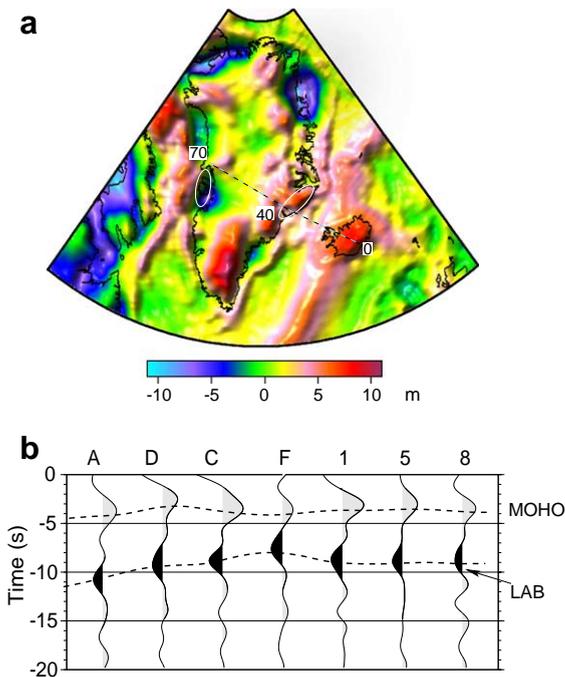

Fig. 8. a) Residual geoid signal in the NW Atlantic region, obtained from a combination of CHAMP and GRACE satellite and aerogravimetry/terrestrial gravity data (after removal of all geoid components >2500 km). The suggested trace of the Iceland plume is marked (dashed line, [43]). The numbers give the estimated time of the plume location in millions years BP. The white encircled regions near the plume track mark Tertiary flood basalts in eastern and western Greenland. b) S-receiver functions from Fig. 5a aligned along the plume trace. The characters on the top of the figure mark the regions described in Figs. 1, 2, and 3a.

Acknowledgements

References

[1] J. Barrell, The strength of the Earth's crust, J. Geol. 22 (1914) 680ff.

[2] D.L. Anderson, Lithosphere, asthenosphere, and perisphere, Rev. Geophys. 33 (1995) 125–149.

[3] B. Gutenberg, Untersuchungen zur Frage bis zu welcher Tiefe die Erde kristallin ist, Z. Geophys. 2 (1926) 24–29.

[4] J. Dormann, M. Ewing, J. Oliver, Study of shear-wave velocity distribution in the upper mantle by mantle Rayleigh waves, Bull. Seismol. Soc. Am. 50 (1960) 87–115.

[5] H. Thybo, E. Perchuc, The seismic 8° discontinuity and partial melting in the continental mantle, Science 275 (1997) 1626–1629.

[6] X. Li, R. Kind, X. Yuan, I. Woelbern, W. Hanka, Rejuvenation of the lithosphere by the Hawaiian plume, Nature 427 (2004) 827–829.

[7] P. Kumar, X. Yuan, R. Kind, G. Kosarev, The lithosphere–asthenosphere boundary in the Tien Shan–Karakoram region from S receiver functions: evidence for continental subduction, Geophys. J. Lett. 32 (2005), doi:10.1029/2004GL022291.

[8] V. Farra, L.P. Vinnik, Upper mantle stratification by P and S receiver functions, Geophys. J. Int. 141 (2000) 699–712.

[9] N. Henriksen, A.K. Higgins, F. Kalsbeek, T.C.R. Pulvertaft, Greenland from archean to quarternary, Geol. Greenl. Surv. Bull. 185 (2000).

[10] F.A. Darbyshire, T.B. Larsen, K. Mosegaard, T. Dahl-Jensen, O. Gudmundsson, T. Bach, S. Gregersen, H. Pedersen, W. Hanka, A first detailed look at the Greenland lithosphere and upper mantle, using Rayleigh wave tomography, Geophys. J. Int. 158 (2004) 267–286.

[11] W.J. Morgan, Convection plumes in the lower mantle, Nature 230 (1971) 42–43.

[12] D.L. Anderson, Thermal state of the upper mantle; no role for mantle plume, Geophys. Res. Lett. 27 (2000) 3623–3626.

[13] F.A. Darbyshire, I.T. Bjarnason, R.S. White, O.G. Flovenz, Crustal structure above the Iceland mantle plume imaged by the ICEMELT refraction profile, Geophys. J. Int. 135 (1998) 1131–1149.

[14] M.A. Allen, G. Nolet, W.J. Morgan, K. Vogfjord, M. Nettles, G. Ekstrom, B.H. Bergsson, P. Erlendsson, G.R. Foulger, S. Jakobsdottir, B.R. Julian, M. Pritchard, S. Ragnarson, R. Stefanson, Plume driven plumbing and crustal formation in Iceland, J. Geophys. Res. 107 (B8) (2002) 2163, doi:10.1029/2001JB000584.

[15] R. White, D. McKenzie, Magmatism at rift zones: the generation of volcanic continental margins and flood basalts, J. Geophys. Res. 94 (1989) 7685–7729.

[16] F. Sigmundsson, Post-glacial rebound and asthenosphere viscosity in Iceland, Geophys. Res. Lett. 18 (1991) 1131–1134.

[17] H.E.F. Amundsen, et al., in: B. Jamtveit, H.E.F. Amundsen (Eds.), 15th Kongsberg Seminar, Norway, Kongsberg, 2002.

[18] I.T. Bjarnason, The Lithosphere and Asthenosphere of the Iceland Hot Spot, IUGG, 2003.

[19] T. Fedorova, W.R. Jacoby, H. Wallner, Crust–mantle transition and Moho model for Iceland and surroundings from seismic, topography, and gravity data, Tectonophysics 396 (2005) 119–140.

[20] I.T. Bjarnason, How thick is the lithosphere below Iceland? How large is the velocity inversion and what does it mean? (Abstract), EOS Trans. AGU 80 (46) (1999) F645 (Fall Meet. Suppl.).

[21] A. Li, R.S. Detrick, Structure of crust and upper mantle beneath Iceland from Rayleigh wave tomography (Abstract), EOS Trans. AGU 84 (46) (2003) F645 (Fall Meet. Suppl.).

[22] J.R. Evans, I.S. Sacks, Deep structure of the Iceland plateau, J. Geophys. Res. 84 (1979) 6859–6866.

[23] L.P. Vinnik, G.R. Foulger, Z. Du, Seismic boundaries in the mantle beneath Iceland: a new constraint on temperature, Geophys. J. Int. 160 (2005) 533–538.

[24] S. Kodaira, R. Mjelde, K. Gunnarsson, H. Shiobara, H. Shimamura, Structure of Jan Mayen microcontinent and implication for its evolution, Geophys. J. Int. 132 (1998) 383–400.

[25] T. Dahl-Jensen, T.B. Larsen, I. Woelbern, T. Bach, W. Hanka, R. Kind, S. Gregersen, K. Mosegaard, P. Voss, O. Gudmundsson, Depth to Moho in Greenland: receiver function analysis suggests two proterozoic blocks in Greenland, Earth Planet. Sci. Lett. 205 (2003) 379–393.

[26] S. Pilidou, K. Priestley, E. Debayle, O. Gudmundsson, Rayleigh wave tomography in the North Atlantic: high resolution images of the Iceland, Azores and Eifel mantle plumes, LITHOS 79 (2005) 453–474.

[27] I.T. Bjarnason, C.J. Wolfe, S.C. Solomon, G. Gudmundson, Initial results from the ICEMELT experiment: body-wave delay times and shear-wave splitting across Iceland, Geophys. Res. Lett. 23 (1996) 459–462, doi:10.1029/96GL00420.

[28] G.R. Foulger, M.J. Pritchard, B.R. Julian, J.R. Evans, R.M. Allen, G. Nolet, W.J. Morgan, B.H. Bergsson, P. Erlendsson, S. Jakobsdottir, S. Ragnarsson, R. Stefansson, K. Vogfjord, The seismic anomaly beneath Iceland extends down to the mantle transition zone and no deeper, Geophys. J. Int. 142 (2000) F1–F5.

[29] R. Butler, T. Lay, K. Creager, P. Earl, K. Fischer, J. Gaherty, G. Laske, B. Leith, J. Park, M. Ritzwoller, J. Tromp, L. Wen, The global seismographic network surpasses its design goals, EOS Trans. AGU 80 (23) (2004) 225–229.

[30] W. Hanka, A. Heinloo, K.-H. Jaeckel, Networked seismographs: GEOPHONE real time data distribution, ORFEUS Electron. Newsl. 2 (2000) 24 (http://orfeus.knmi.nl/newsletter/vol2no3/heofon.html).

[31] J. Fyen, K. Iranpour, Near real time data at NORSAR for CTBT monitoring, ORFEUS Electron. Newsl. 5 (2) (2003) (http://orfeus.knmi.nl/newsletter/vol5no2/norsar.html).

[32] B.L.N. Kennett, E.R. Engdahl, Traveltimes for global earthquake location and phase identification, Geophys. J. Int. 105 (1991) 429–465.

[33] F. Sigmundsson, P. Einarsson, Glacial-isostatic crustal movements caused by historical volume change of the Vatnajoekull ice cap Iceland, Geophys. Res. Lett. 19 (1992) 2123–2126.

[34] M. Thoma, D. Wolf, Inverting uplift near Vatnajoekull, Iceland, in terms of lithosphere thickness and viscosity stratification, in: M. Sideris (Ed.), Gravity, Geoid and Geodynamics, Springer-Verlag, Berlin, 2001, pp. 97–102.

[35] L. Sjoeberg, M. Pan, E. Asenjo, S. Erlingsson, Glacial rebound near Vatnajoekull, Iceland, studied by GPS campaigns in 1992 and 1996, J. Geodyn. 29 (2000) 63–70.

[36] G.R. Foulger, C.-H. Jahn, G. Seeber, P. Einarsson, B.R. Julian, K. Heki, Post-rifting stress relaxation at the divergent plate boundary in Iceland, Nature 358 (1992) 488–490.

[37] F.F. Pollitz, I.S. Sachs, Viscosity structure beneath northeast Iceland, J. Geophys. Res. 101 (1996) 17771–17779.

[38] L.E. Sjoeberg, M. Pan, S. Erlingsson, E. Asenjo, K. Arnason, Land uplift near Vatnajoekull, Iceland, as observed by GPS in 1992, 1996 and 1999, Geophys. J. Int. 159 (2004) 943–948.

[39] M. Storey, A.K. Pedersen, O. Stecher, S. Bernstein, H.C. Larsen, L.M. Larsen, J.A. Baker, R.A. Duncan, Long-lived postbreakup magmatism along the east Greenland margin: evidence from shallow-mantle metasomatism by the Iceland plume, Geology 32 (2004) 173–176, doi:10.1130/G19889.1.

[40] C. Reigber, H. Jochmann, J. Wünsch, S. Petrovic, P. Schwintzer, F. Barthelmes, K.-H. Neumayer, R. König, C. Förste, G. Balmino, R. Biancale, J.-M. Lemoine, S. Loyer, F. Perosanz, Earth gravity field and seasonal variability from CHAMP, in: C. Reigber, H. Lühr, P. Schwintzer, J. Wickert (Eds.), Earth Observation with CHAMP—Results from Three Years in Orbit, Springer-Verlag, Berlin, 2004, pp. 25–30.

[41] C. Reigber, R. Schmidt, F. Flechtner, R. König, U. Meyer, K.-H. Neumayer, P. Schwintzer, S.Y. Zhu, An Earth gravity field model complete to degree and order 150 from GRACE: EIGEN-GRACE02S, J. Geodyn. 39 (2005) 1–10.

[42] R.S. Forsberg, Kenyon, Gravity and geoid in the Arctic region—The northern gap now filled, Proc. of 2nd GOCE User Workshop (on CD-ROM), ESA SP-569, ESA Publication Division, 2004.

[43] L.A. Lawver, R.D. Müller, Iceland hotspot track, Geology 22 (1994) 311–314.